Significant decline of mesospheric water vapor at the NDACC site Bern in the period 2007 to 2018

Martin Lainer (on behalf of all co-authors)

Response to comments on ACPD paper acp-2018-711

Color Code: Referee comments, Authors response, Proposed changes in manuscript

---

We would like to thank all anonymous referees and the Editor for their constructive comments to our discussion paper.

Please find our point by point responses to the reviewers for the first revision stage below, together with our suggestions to change the manuscript. At the end we included a marked-up version of the updated manuscript.

1 Response to Referee #1

The study presents a trend analysis of the 10-year data set of middle atmospheric water vapor measured by a ground based microwave radiometer. It is emphasized that the measurement does not show any drifts despite some hardware upgrades and changes in the calibration cycle. Significant trends are found in the mesosphere and upper stratosphere.
The paper addresses an important topic and makes potentially a valuable contribution. However, major revisions are needed to present the necessary evidence, that the measurement does not show significant drifts. The analysis of the baseline is not convincing since it is rather an analysis of the noise instead of the baseline. Changes in the noise level are evident and its consequences on the measurement not sufficiently discussed. The data set does not seem to be homogenized. Despite a dynamic integration scheme to keep the noise level constant there are important variations in the measurement response. The test of the stability of the averaging kernels is over stressed and does not prove that there is no drift in the measurement.

- The analysis of the baseline as stated in the manuscript is indeed at a first instance an analysis of the measurement noise. However, indirectly we show the good stability of the baseline fitting in the retrieval algorithms. The changes in noise patterns are visible in the 3-dimensional view, but very tiny and would not be recognizable in a 2-dimensional plot looking from above. We do not see any severe changes in noise levels, only small patterns originating either from temperature fluctuations or changes in tropospheric attenuation of the line signal or a combination of both.

- Homogenization would have been necessary if for example a replacement of the spectrometer would have taken place. But did not. Only adjusting the measurement cycle and installing a faster mirror motor does not imply to do a homogenization.

- The periodically variations of the measurement response (Fig. 1) originate from the seasonal variability of the H_2O line strength. We note that these changes in the measurement response do not seem to be important for the trend, because the a priori (MLS) information does not have any trend.

- We think the AVK test is the best way to show the stability of the water vapor measurements. Any important drift of the measurements would be reflected in the AVK development.

The Introduction is focused on troposphere and stratosphere but the main results are in the mesosphere. Please adapt the focus of the introduction.

- We think that some kind of broader introduction to the topic is useful for the reader. Therefor we would like to keep the information on the upper troposphere and stratosphere.

P4/l6: this is not the SNR but the noise.

- Yes this is correct and we will change the expression.

- Page 4, line 6: Corrected expression "signal to noise ratio" by "the measurement noise".

P4/l14: with 80 MHz bandwith there is no sensitivity at 10 hPa. Hence the difference simply refers to the difference between MLS climatology (a priori) and MLS measurements. Further, it would be interesting to know, if the bias of 10% towards MLS is constant over time?

- Regarding the sensitivity at 10 hPa, we are refering to Lainer et al. (2015), where a retrieval version of 225 MHz bandwidth is used. For stability reasons we only use 80 MHz in this trend study. So the difference statement is still correct. Although data down to 10 hPa is shown, we do not make use of it in the results.

- Regarding the bias evolution to MLS over time, we refer to the answer given to a similar comment of referee #3 in Sec. 3.2.2.

P4/l16: Figure 1 does not show anything about the stability of the baseline but only about the evolution of the measurement noise. To demonstrate the stability, please show the annual averages of the residuals instead.

- Thank you very much for this important hint. It is true, we show the evolution of the residuals. But indirectly we show that our baseline fitting works well, otherwise the residual patterns would be not centered at the zero value.
- With the histograms we already show the good stability of the noise, confirming also that the baseline removal works well.
- We will update the manuscript regarding Figure 1 and state that we show the residual development. Fig. 1 shows that there is no drift in the residuals. It also indicates that we correctly removed the baseline.
- We correct all statements involving the baseline. And we clarify that the residuals do not show a drift. This is due to the correct fitting of the baseline and to the stability of the radiometer.

The annual cycle that is visible in Figure 1 contradicts the statement on p4/l6 that the variable integration time ensures a constant noise level. The explanation given on p5/l1 do not apply since the variable integration time should account for all such effects. Further, it is not precise to say the SNR is constant, since if the noise is kept constant with dynamic integration, the line strength can still vary and modify the SNR. The change in pattern after 2016 have to be discussed as well.

- The 3D view of Figure 1 shows very tiny residual patterns that would not be visible if one looks from above (2D view) onto the plot. Also the histograms confirm that the residuals are very constant over the years.
- To clarify the noise issue, we note, that with the variable inegration time we keep the thermal noise of the measured difference spectrum constant at 0.01 K.
- It is true, that we analyse the residuals which are most important to show the goodness of the retrieval.

P5/l2: I do not agree with the statement that such changes do not affect the retrieval. Changes in the measurement noise affect the sensitivity of the retrieval and can in turn affect the trend analysis.

- Sure, the thermal noise affects the sensitivity of the retrieval, but we keep it constant. Figure 1 is showing the residuals, not the noise itself. Those 2 things should be separated. The white lines in Fig. 2 confirm that the noise level is not drifting. There are periodically patterns, but no up/down trends. We are convinced that this does not effect the trend analysis since the trend model includes an annual oscillation and its harmonics.

P5/l14: Why does the white line show such a pronounced seasonal cycle if the measurement error is supposed to be kept constant?

- It is not the measurement error that is kept constant, but the thermal noise. The line strength changes over the year (annual cycle) due to changing tropospheric attenuation. This makes the measurement response or apriori contribution (white line) change periodically with time.

P5/l21: if the observational error is essentially a statistical error, should it not decrease when calculating the monthly mean? Hence why is not $\sigma_{obs}/sqrt(N)$ the correct value?

- We account for the increased sample number within the computation of the standard error $\sigma_{std} = \sigma/sqrt(N)$.

P5/l29: For dataset shorter than one solar cycle, the solar cycle (SC) term can be highly correlated with the linear term and should be avoided. Are the SC and the linear term correlated in this trend study? What would be the trend results without the SC proxy?

- The inclusion of the solar cycle term is essential for the trend model since upper mesospheric water vapour is sensitive to photolysis by the Lyman-alpha radiation of the sun. The uncertainty of the trend estimate inclusive of the solar cycle term is fully considered by the error analysis. Thus, there is no need to switch off the solar cycle term in the trend model since the trend estimate would be of reduced quality if the solar cycle term is not included.

P6/l29: the test with the AVK is much appreciated and a very good indication for the good quality of the data set. However, it does not prove, that there is no shift/steps in the data set which could arise for instance form a drift in frequency. Please comment.

- There are no indications of a drift of the radiometer. Such a drift is avoided by the tipping curve calibration. The frequency-channel relationship is constant since we operate a FFT spectrometer where the spectrum is digitally analysed.

P8/l5: positive drift detected by Hurst et al on MLS are at a pressure levels of greater than 20 hPa. The authors cannot justify the difference between MIAWARA and MLS trends in the low mesosphere by this drift.

- Regarding our manuscript, we do not justify anything by the study of Hurst et al. (2016). Maybe there is mis-understanding. On page 8, lines 9-10, we only state that "However, Aura/MLS H_2O data could be problematic for estimating trends due to detected data drifts (Hurst et al., 2016)."

- We can add the corresponding pressure levels: "below 20 hPa" to this sentence to clarify.

- Page 8, line 10: Added "..below 20 hPa..".

P8/l11: I do not agree:

- Stability of the baseline has not been shown, see comment above.
- It has been shown, that the actual AVKs do not introduce a drift. It has not been shown that the instrument has no drift. More evidence would be helpful to convince the reader.

- We will adapt the text and say that we have shown the evolution and good stability of the measurement noise (only tiny changes, patterns) and with that the functioning of the baseline fitting.
- We are convinced that the AVK is one of the best variables to show the stability of a measurement time series from a radiometer. If the measurements of MIAWARA would drift, the AVK's would also drift. And we have shown that the AVK's are not drifting.

2 Response to Referee #2

The paper is interesting, important, well written and fulfills the requirements for ACP. Referee: 3 has given valuable comments that I support. I would also like the authors to add a km altitude scale to the right of figures 2 and 4.

- Sure, it is a good idea to include also a km altitude scale to Fig. 4, because we also give references in km in the text for this figure. However, for Fig. 2 we did not include it because their is no reference in km given in the text. The pressure altitude nomenclatur is typically used for plots covering the middle atmosphere.

- We added km altitude scales to Fig. 4 on the right hand side of the plots.

3 Response to Referee #3

3.1 General point

I am not convinced that the fitted time model of Equation 2 is good. The figure on this topic, Figure 3, has a yearly variation from 4 ppmv to 8 ppmv in the altitude range the authors selected to show. The residual is about 1 ppmv, up and down to 0.5 ppmv, or 12-25% of the total volume mixing ratio. This is a lot, especially as the authors find a decadal trend that is of equal or smaller magnitude than the residuals. The authors need to justify these residuals, identify where they are from, and clearly limit the error range of the time model.

- We cannot agree to this statement. First, the fitted time model in Equation 2 is a well established method (von Clarmann et al., 2010) and was successfully used in other middle atmospheric trend studies (Moreira et al., 2015) before. The Referee's concern about the residual between measurements and fit is seen from a wrong direction. It is true that locally the residual can reach about 0.5ppm, so maximal 6-12% of the total VMR. However no drift in the residual is present and the mean over the investigated time series is very low (-0.003 ppm). This shows already that the time model fit does a very good job. In our point of view no additional improvements to limit the error range of the time model is neccessary. Regarding ozone residuals shown in Fig. 7 by Moreira et al. (2015), they even reach higher values up to 1ppm, which is still not a problem for retrieving meaningful trends.

- At a first instance, we have not changed the manuscript. See answer above to first comment of Referee.

3.2 Specific points

3.2.1 About Equation 2, the time series

In Figure 3, the fit seems much more regular over the years than the gathered data. This might be because there are large uncertainties allowed in the fitting mechanism, or because the fit is simply not good. What are the computed uncertainties? Please give error bars in Figure 3.

- That the model fit is more regular and smoother than the data is expected. The fit in our opinion is quite good and represents well the long-term variability of the measurements. Overall the regression model explains about 90 % of the variance between 0.02 and 3 hPa.

- In the manuscript we added the statement that the regression model explains about 90 % of the variance between 0.02 and 3 hPa.

How are you sure that $F_{10.7}$, the multivariate ENSO index, and the quasi-biennial oscillation phase shift, all only have linear influence on water vapor volume mixing ratios?

- We agree that a nonlinear response of the water vapour volume mixing ratios to the solar cycle, ENSO and QBO is possible. However, an investigation of nonlinear effects exceeds the aim of our trend study.

What happens to the fit if you switch from monthly to weekly, daily, or a by-the-measurements time series?

- By now the used trend model only allows to input monthly mean data sets. So this question cannot be answered in a short time. A future program release might allow to check this, but this is defenitly beyond our influence at the moment.

- At the moment and the current setup of our investigation, we are not able to include such an investigation. No changes made.

Using c_n/d_n and already having defined c_1 and d_1 is confusing. Also, by your own definitions on page 6 line 24, you never fit semi-annual or annual changes. This does not seem as intended. Can you define m, and which l_n you use more precisely? And why limit yourself to just annual and semi-annual trends immediately without decomposing these frequencies from the data first? It is perfectly reasonable to have weather trends that are not exactly annual during such short times as 11 years. And because of the QBO, even lower frequencies seems reasonable to find as well.

- Yes, we agree this is a bit confusing and will be clarified in the manuscript. We will define the used l_n and m and correct our definition on page 6, line 24. We fit semi-annual and annual changes, so the sum term goes from n=2 to m=3. The major contribution comes from the semi-annual, respectively annual variation. We agree that other periodicites could be present in the data as well, but since our time model fit in our opinion is already very good, considering other periodicities (expecially shorter than semi-annual) would not impact the trend result a lot and can be neglected.

- An analysis of the dominant frequencies is not necessary since the residuals of our trend model in Fig. 3 are small and do not contain a dominant frequency component.

- Equation 2: We improved the readability of the regression function by changing m to the value 3. Page 6, line 24: Included c_3, c_4, d_3 and d_4, the coefficients for the semi-annual and annual variability. We also defined l_n (the period length) more precisely.

Please confirm that the added extra month that makes the time series 11 years and 1 month long has no impact on your results. Its a minor thing, but with such a poor fit, and with the sharp increase of water vapor there is in Figure 3 around April/May, a single outlier like this can be bothersome.

- Regarding this extra month, we want to notice that we do not see a very sharp increase in VMR at the end of Fig. 2. However to be more quantitative, during the analysis and preparation for this study we piecewise increased the water vapor data time series and made the respective trend calculations as time went by. The impact of the included extra month (April 2018) on the trend estimate was found to be very small (changed the trend estimate less than 0.05ppm). We will notice this finding in Section 3.2.

- Page 8, line 6: Here we add the statement, that the additional month does not behave like an outlier. It does not change the trend estimate results.

3.2.2 About a priori and retrieval model constraints

Why the large area for the a priori? You point north, so the southern tip of said area is at your instrument site? Are the coincidences evenly distributed in said area?

- We are not completely sure about what this comment is about. We choose a 400x800km area around the groumd-based measurements site where we calculate mean satellite profiles for comparison. Within this area 2 EOS Aura overpasses per day take place. For the a priori we take something different, exactly a monthly mean zonal mean climatology.

You have a 10% difference between your own measurements and those of Aura/MLS. Are these differences constant over the years?

- Within the paper by Nedoluha et al. (2017) compares annual average differences between coincident H_2O measurements and MLS at 0.46hPa for 6 ground-based sites including Bern (MIAWARA). At this altitude MIAWARA data does not behave worse than other ground based data between 2007 and 2014. Usually it is easier to keep ground-based measurements more stable than satellite data. Thus GB data is often used to validate satellite data.

There was a recent conference proceedings paper by Rosenkranz et al (10.1109/MICRORAD.2018.8430729) about model errors in the microwave range due to both errors in spectroscopic parameters and the correlation between these errors due to how they are derived in the lab. You never explicitly say so, but I presume you are using his model for the molecular oxygen absorption and possibly even for water in said range, so it seems relevant. If so, the recent paper's findings are important, and they are that there is potential brightness temperature errors of between 0.5 and 1 K in and around the water line you are measuring. What would taking this into account do for your retrievals? Also, please give and cite the spectroscopic model you are using, since this is a user option in ARTS/Qpack.

- As spectroscopic model we use a combination of the H2O-MPM93 model from Liebe et al. (1993) (for the pressure broadened half line width) and recent entries in the JPL (Jet Propulsion Laboratory) line catalog for the lower state energy and line strength at 300 K.

- Page 3, line 22 ff: We give the above information about the spectroscopic H_2O model as a reference in the text: "As spectroscopic H_2O model a combination of the H2O-MPM93 model from Liebe et al. (1993), for the pressure broadened half line width, and recent entries in the JPL (Jet Propulsion Laboratory) line catalog, for the lower state energy and line strength at 300 K, is taken."

3.2.3 About the water measurements

Please give specific examples of the fits of Figure 1 for the change that happens around 2011 and explain why you don't believe changing your setup affects the quality of the retrievals from these figures. I can guess you have some sort of standing wave that you can remove in post via periodograms or whatever your favorite deconvolution method might be. I do not think I should be guessing these things though, since it makes the study less repeatable. So a couple of plots with the measured and fitted line in the center, and an explanation why it is clear that the results are the same both pre- and post-2011 in terms of water vapor would help.

- In Figure 1 the residuals shown and have tiny fluctuation patterns. However the thermal noise of the observed spectra is kept constant at 0.01 K. Theoretically changes in the level of thermal noise would indeed affect the retrieval, thus we keep it constant guaranteeing a stable retrieval performance.
- We will give more details on our baseline fitting method. We apply a polynomial fit of fifth order and a sinus fit with 6 coefficients to our calibrated spectrum. The sinus fit is done by an internal MatLab fitting routine.
- The visible change in residual fluctuation patterns after 2011 is only due to the increased sample size of measurements. The actual T_R peak amplitudes pre- and post 2011 are the same.
- Page 4, line 19ff: We added a sentence on the baseline fitting methods applied. "Overall two differnt baseline fittings are performed. A polynomial fit of fifth order and a sinus fit with 6 coefficients guarantee a stable removal of baseline artefacts on our calibrated spectra".

3.3 Technical notes

The entire discussion about ozone in the introduction is irrelevant for the rest of the paper. Please remove it.

- This section about ozone could be deleted, but maybe it is still of interest for the reader, because we also describe trend studies that used the same trend model.

Equation 3 should not use y since it is already used in Equation 2. Please change either one of these equations.

- Ok we agree and will change the small y in Equation 2 to a uppercase Y.
- Equation 2: Changed $y(t)$ to $Y(t)$.

Please give all the fitted parameters for Equation 2 in a table or in a figure for different altitudes.

- Such a table would be rather confusing and of limited value since the fitted parameters are different at each pressure level.

- All paper May as such and not Mai.
- Page 1 line 15. Please reformulate the first sentence to clarify what is characterizing what and how it is characterizing it. I can guess what you mean but it is unclear.
- Page 1 line 21. Please tell for what year the $0.05\,\mathrm{W\,m^{-2}}$ is from.
- Page 3 line 3-4. Please cite and give the full name of each instrument.
- Page 7 line 25: according.

- Thank you for those comments, which will be considered as far as possible in the revised manuscript.
- Ragarding page 1, line 21: This number is an average between 1999 and 2016, and not for a specific year.
- We agree to give full instrument names, but no citations, since it is already information from another citation Nedoluha et al. (2017).
- Changed Mai to May troughout the manuscript.
- Page 1, line 15: Adjusted sentence for better understanding.
- Page 1, line 21: Now: Globally averaged (1999 to 2016)...
- Page 3, line 3-4: Full names of each instruments are givem.
- Page 7, line 25: Changed to "According"

References

Lainer, M., Kämpfer, N., Tschanz, B., Nedoluha, G. E., Ka, S., and Oh, J. J. (2015). Trajectory mapping of middle atmospheric water vapor by a mini network of ndacc instruments. *Atmospheric Chemistry and Physics*, 15(16):9711–9730.

Liebe, H., Hufford, G., and Cotton, M. (1993). Propagation modeling of moist air and suspended water/ice particles at frequencies below 1000 ghz. In *In AGARD, Atmospheric Propagation Effects Through Natural and Man-Made Obscurants for Visible to MM-Wave Radiation 11 p (SEE N94-30495 08-32)*.

Moreira, L., Hocke, K., Eckert, E., von Clarmann, T., and Kämpfer, N. (2015). Trend analysis of the 20-year time series of stratospheric ozone profiles observed by the gromos microwave radiometer at bern. *Atmospheric Chemistry and Physics*, 15(19):10999–11009.

Nedoluha, G. E., Kiefer, M., Lossow, S., Gomez, R. M., Kämpfer, N., Lainer, M., Forkman, P., Christensen, O. M., Oh, J. J., Hartogh, P., Anderson, J., Bramstedt, K., Dinelli, B. M., Garcia-Comas, M., Hervig, M., Murtagh, D., Raspollini, P., Read, W. G., Rosenlof, K., Stiller, G. P., and Walker, K. A. (2017). The sparc water vapor assessment ii: intercomparison of satellite and ground-based microwave measurements. *Atmospheric Chemistry and Physics*, 17(23):14543–14558.

von Clarmann, T., Stiller, G., Grabowski, U., Eckert, E., and Orphal, J. (2010). Technical note: Trend estimation from irregularly sampled, correlated data. *Atmospheric Chemistry and Physics*, 10(14):6737–6747.

Significant decline of mesospheric water vapor at the NDACC site Bern in the period 2007 to 2018

Martin Lainer[1], Klemens Hocke[1], Ellen Eckert[2], and Niklaus Kämpfer[1]

[1]Institute of Applied Physics, University of Bern, Bern, Switzerland
[2]University of Toronto, Department of Physics, 60 St. George Street, Toronto, Ontario M5S 1A7, Canada

Correspondence: Martin Lainer (martin.lainer@iap.unibe.ch)

Abstract. The middle atmospheric water vapor radiometer MIAWARA is located close to Bern in Zimmerwald ($46.88°$ N, $7.46°$ E, $907\,\mathrm{m}$) and is part of the Network for the Detection of Atmospheric Composition Change (NDACC). Initially built in the year 2002, a major upgrade of the instruments spectrometer allowed to continuously measure middle atmospheric water vapor since April 2007. Thenceforward to ~~Mai~~ May 2018, a time series of more than 11 years has been gathered, that makes a first trend estimate possible. For the trend estimation, a robust multi-linear parametric trend model has been used. The trend model encompasses a linear term, a solar activity tracker, the El Niño–Southern Oscillation (ENSO) index, the quasi-biennial oscillation (QBO) as well as the annual and semi-annual oscillation. In the time period April 2007 to ~~Mai~~ May 2018 we find a significant decline in water vapor by $-0.6 \pm 0.2\,\mathrm{ppm\,decade^{-1}}$ between 61 and $72\,\mathrm{km}$. Below the stratopause level ($\sim 48\,\mathrm{km}$) a smaller reduction of H_2O of up to $-0.3 \pm 0.1\,\mathrm{ppm\,decade^{-1}}$ is detected.

1 Introduction

Water vapor is the most important greenhouse gas in the atmosphere (Kiehl and Trenberth, 1997) and has a dominant feedback role in the Earth's climate system. In the troposphere it provides the main source of moisture for the formation process of precipitation in the atmosphere. While global warming progresses, the amount of moisture is expected to increase faster than the overall amount of precipitation, that is controlled by evaporation and the heat budget at the surface (Trenberth et al., 2003).

~~Changes in~~ Long-term changes in the abundance of atmospheric water vapor can be used to characterize climate change. One region of the atmosphere which is very sensitive to those changes is the upper troposphere, but the actual impact on climate change is poorly understood (Held and Soden, 2000). Some direct anthropogenic changes in water vapor are due to emissions by aviation and the possible subsequent formation of contrails that freeze-dry the air and exert a strong radiative forcing (RF) effect. Contrails that persist for several hours and loose their line shaped form are known as contrail-cirrus. Globally averaged (1999 to 2016), annual mean RF estimates with uncertainty ranges are about 0.01 (0.005-0.03) $\mathrm{W\,m^{-2}}$ for long-lived contrails alone, and together with contrail-cirrus RF reaches about 0.05 (0.02-0.15) $\mathrm{W\,m^{-2}}$ (Kärcher, 2018). In contrast, total aviation RF for instance in the year 2000 is about $0.048\,\mathrm{W\,m^{-2}}$ (Sausen et al., 2005).

Compared to the troposphere, the stratosphere is very dry and the amount of H_2O is commonly indicated in volume mixing ratios (parts per million) like for ozone. Water vapor from the troposphere can enter the stratosphere mainly through convective

processes at the equator. The cold tropical tropopause acts as a cold trap for ascending tropospheric air and causes most of the water vapor to freeze out. Nevertheless, water vapor in the stratosphere has a high impact on ozone chemistry and it is of importance to a global warming feedback process. Further, water vapor provides the main source of hydrogen radicals (OH, H, HO_2), which are involved in the catalytic destruction cycle of ozone in the stratosphere (Brasseur and Solomon, 2006). An important long-term data set of lower free tropospheric ($2\,\mathrm{km}$) up to middle stratospheric ($28\,\mathrm{km}$) water vapor is available from Boulder (Colorado) since 1980. This data comes from balloon frost-point hygrometer (FPH) measurements that are launched usually once per month. A weighted, piecewise regression analysis of the 30-year record from 1980 to 2010 by Hurst et al. (2011) revealed an average increase by $1.0 \pm 0.2\,\mathrm{ppm}$ in the altitude range between 16 and $26\,\mathrm{km}$. About a quarter of the H_2O increase could be attributed to changes in the methane (CH_4) concentration. Methane can easily be transported from the surface upward into the stratosphere where its oxidation is a major in-situ source of water vapor.

Compared to water vapor, stratospheric ozone gathered much higher scientific attention in regard of its long-term development after the detection of the Antarctic ozone whole in 1985 (Farman et al., 1985). Two years later in 1987 the Montreal Protocol has been signed to protect the ozone layer by banning and regulating the production of numerous substances that are responsible for ozone depletion. Numerous trend studies on ozone were published in the past years (e.g. Eckert et al., 2014; Moreira et al., 2015; Steinbrecht et al., 2017; Ball et al., 2018) showing how ozone developed in the course of time. Drift-corrected ozone trends from MIPAS (Michelson Interferometer for Passive Atmospheric Sounding) space-borne observations (July 2002 to April 2012) range from negative (up to $-0.41\,\mathrm{ppm\,decade^{-1}}$) in the tropical stratosphere to positive ($+0.55\,\mathrm{ppm\,decade^{-1}}$) at southern mid-latitudes (Eckert et al., 2014). A 20-year continuous mapping of the stratospheric ozone layer at the NDACC site Bern could be achieved. A recent trend analysis by Moreira et al. (2015) showed that ozone recovered by about $3\,\%\,\mathrm{decade^{-1}}$ at an altitude of $40\,\mathrm{km}$ within the time period 1997 to 2015. Steinbrecht et al. (2017) calculated ozone trends for larger number of ground-based NDACC site observations by different techniques such as FTIR (Fourier-Transform-Infrared-Spectrometer), microwave radiometry or lidar. They found positive trends between 35 and $48\,\mathrm{km}$ altitude in the tropics as well as in the the 35 to 65°latitude bands of the Northern and Southern Hemisphere. More specifically, ozone mixing ratios at $42\,\mathrm{km}$ increased by 1.5 (tropics) and 2-2.5 (mid-latitudes) $\%\,\mathrm{decade^{-1}}$, respectively. Although total column measurements of ozone show that the ozone layer stopped to decline across the globe, there is some evidence from satellite observations that lower stratospheric ozone continued to decline within $60°\,\mathrm{N}$ to $60°\,\mathrm{S}$ after 1998, resulting in downward trend of stratospheric ozone columns (Ball et al., 2018).

In order to understand detected water vapor trends in the middle atmosphere, models and measurements are both important. A 40-year (1960-1999) model simulation with the coupled chemistry-climate model (CCM) ECHAM resulted in a global mean stratospheric H_2O increase by $0.7\,\mathrm{ppm}$ between 1980 and 1999 (Stenke and Grewe, 2005). Trend estimates in lower stratospheric water vapor strongly differentiate between the NOAA (National Oceanic and Atmospheric Administration) FPH observations at Boulder and merged zonal mean satellite measurements as pointed out by Lossow et al. (2018). The differences reach up to $0.5\,\mathrm{ppm\,decade^{-1}}$ and change the signs from positive for the in-situ observations to negative for the processed satellite data. But not only the observations do not agree, also extensive trend estimates from simulations show discrepancies for the location of Boulder and the corresponding zonal mean latitude band around $40°\,\mathrm{N}$. An intercompari-

son of ground-based microwave and satellite linear trends in the lower mesosphere at an altitude of about 53 km (0.46 hPa) within different extended periods shows no consistent picture between the different observations. The following stations were considered in the study by Nedoluha et al. (2017): Lauder, Mauna Loa, Table Mountain, Seoul, Bern and Onsala. Satellite retrievals that were integrated in the intercomparison include ACE-FTS ~~, HALOE, MIPAS, MLS, SCIAMACHY, SMR, SOFIE~~ (Advanced Composition Explorer - Fourier Transform Spectrometer), HALOE (Halogen Occultation Experiment), MIPAS (Michelson Interferometer for Passive Atmospheric Sounding), MLS (Microwave Limb Sounder), SCIAMACHY (Scanning Imaging Absorption Spectrometer for Atmospheric Chartography), SMR (Sub-Millimeterwave Radiometer), SOFIE (Solar Occultation For Ice Experiment) and different data subversions of those. At none of the comparison sites a uniform result of only positive or negative trends could be retrieved. This might be related to the problem that the time periods cover different ranges. Regarding Fig. 8 in Nedoluha et al. (2017) the trends at Bern range from $+16$ to $-5\,\%\,\mathrm{decade}^{-1}$. However, the majority of H_2O time series, including Aura/MLS, exhibit small positive relative trends in the range 1-7 $\%\,\mathrm{decade}^{-1}$. At the 0.46 hPa pressure level the multi-linear regression model used in our study does not produce a significant trend at the 95 % confidence level.

Still it is unclear how mesospheric water vapor develops in a changing climate. Therefore it is very important to continue the observations especially from those instruments that already have long records such as the microwave NDACC instruments at Mauna Loa (Hawaii), Table Mountain (USA) or Bern (Switzerland). In this study we report on a detected decline of H_2O in the mesosphere from the NDACC ground-based microwave measurement site Bern in the time period between 2007-2018.

Section 2 introduces the NDACC measurement site Bern with the MIAWARA radiometer in more detail and presents the water vapor data set that is processed in the trend model which is introduced in Sect. 3 later. The final results of the trend study are handled in Sect. 3.2, while conclusions are given in Sect. 4.

2 The MIAWARA radiometer

The MIddle Atmospheric WAter vapor RAdiometer (MIAWARA) measures the intensity of the pressure broadened emission of H_2O molecules at a center frequency of 22.235 GHz (Kämpfer et al., 2012). Atmospheric pressure decreases exponentially with altitude and this information is reflected in the H_2O line shape. The obtained spectra are used to retrieve water vapor profiles by means of radiative transfer calculations and the Optimal Estimation Method as described in Rodgers (2000) using the retrieval software package ARTS/qpack (Eriksson et al., 2005; Buehler et al., 2018). As spectroscopic H_2O model a combination of the H2O-MPM93 model from Liebe et al. (1993), for the pressure broadened half line width, and recent entries in the JPL (Jet Propulsion Laboratory) line catalog, for the lower state energy and line strength at 300 K, is taken. MIAWARA is continuously operated on the roof of the building for Atmospheric Remote Sensing in Zimmerwald (46.88° N, 7.46° E, 907 m a.s.l.), which is close to Bern, since September 2006. The reason why we only use data since April 2007 is a major upgrade of the instrument from optoacoustic to Fast Fourier Transform (FFT) spectrometry. In the course of this upgrade the spectral resolution increased from 600 to 61 kHz. Other technical instrumental parameters are summarized in Table 1.

Table 1. MIAWARA technical specifications

Calibration	Tipping curve and balancing calibration
Operational mode	SSB* 50 dB suppression
Line of view	$\sim$ 20°elevation (northward)
Mirror	Plane aluminum mirror
Antenna	Corrugated horn (HPBW**: 6°)
Receiver temperature	$\sim 180\,\mathrm{K}$
Spectrometer	Aqiris FFTS
Total bandwidth	1 GHz
Spectral channels	16385

*single sideband | ** half power beamwidth

In the last years, data from the MIAWARA radiometer was used to detect a solar induced variability of mesospheric H_2O (Lainer et al., 2016), further it was used to investigate planetary 16-day, sub-diurnal and 2-day atmospheric wave activities by using H_2O as a dynamical tracer (Scheiben et al., 2014; Lainer et al., 2017, 2018).

2.1 Measurement stability

The total spectrometer bandwidth is 1 GHz, but only a narrow part of maximal 250 MHz is in general usable in the retrieval procedure due to baseline artifacts at the wings of the H_2O spectrum. However, the reduced bandwidth is sufficient for the retrieval of water vapor in the middle atmosphere and even less is needed for the mesosphere. In order to guarantee a high stability of the spectral measurements we further constrain the bandwidth to 80 MHz around the central frequency of MIAWARA. Changes in tropospheric opacity due to local weather variability affects the sensitive altitude region of the water vapor profile retrieval. In order to make the retrieved data independent of environmental conditions, we use a special H_2O retrieval with a variable integration time of the spectral information to reach a constant ~~signal to noise ratio~~ measurement noise (0.01 K) of the water vapor spectra. Further, we set the measurement response to 80 % to derive a quite stable upper and lower limit of the measurements. This approach generates profiles with a time resolution of typically a few hours in winter and up to 1-2 days during summer.

The a priori water vapor information is derived from a monthly mean zonal mean climatology using Aura/MLS v2.2 data over 4 years between 2004 and 2008. The most recent Level2 Aura/MLS data (v.4.2) are used to initialize pressure, temperature and geopotential height within the MIAWARA H_2O retrieval. The vertical resolution of the instrument varies between 11 km in the stratosphere and 14 km in the mesosphere (Deuber et al., 2005). An instrument validation against Aura/MLS v3.3 with more than 1000 seasonal separated profile comparisons can be found in Lainer et al. (2015). An area of 800×400 km (E/W $\times$ N/S) has been used as spatial coincident criterion for the satellite overpasses. In the pressure range of 2-10 hPa the relative differences are below 3 % and between 0.05-2 hPa the analysis revealed negative biases of MIAWARA compared to Aura/MLS of up to -10 %.

With Fig. 1 we show the overall development of the MIAWARA ~~baseline with~~ residuals in a bandwidth of 80 MHz. ~~In our case the baseline is~~ The shown residuals are defined as the difference between the observed difference spectrum and the modeled spectrum from the retrieved profile and is illustrated as residuum brightness temperature fluctuations T_R. Especially measurements at lower altitudes like in the stratosphere are particularly dependent on a good baseline ~~stability~~ fitting over a broad frequency range. Overall two differnt baseline fittings are performed. A polynomial fit of fifth order and a sinus fit with 6 coefficients guarantee a stable removal of baseline artefacts on our calibrated spectra.

The 3-D top plot in Fig. 1 shows the time series of T_R from April 2007 to ~~Mai~~ May 2018 in the frequency range 22.195 to 22.275 GHz. Whereas the structure along the time axes changes, a uniform distribution in the frequency domain is predominant. Starting from autumn 2010 the ~~baseline~~ T_R signature changes due to a hardware and measurement cycle upgrade, that made it possible to retrieve H_2O profiles in a higher temporal resolution while maintaining the same ~~signal to noise ratio~~ thermal noise level of the measured difference spectrum. The upgrade of the measurement cycle had no effect on the overall homogeneity of the water vapor time series, also because the measurements were always conducted with the same FFT spectrometer. Since no critical parts of the instrument's receiver chain were replaced in the investigated time period, a thorough homogenization of the data has not been computed for this investigation. The band-like structure in the ~~plot could be a seasonal cycle signature and is maybe~~ residuals is a very tiny pattern and hardly visible in a 2-dimensional plot. The pattern is likely related to temperature changes within the instrumental signal path, like microwave absorbers that are operated at the ambient temperature or periodically changes in the tropospheric attenuation affecting the H_2O line strength. However, the T_R differences that make the band-structure are very small (below $1 \cdot 10^{-2}$ K) and ~~have no effect on~~ will not effect the water vapor retrieval and the trend estimation.

In particular the histograms below the 3-D plot show the PDF (probability density function) of the binned (bin width: $5 \cdot 10^{-3}$ K) brightness temperature fluctuations T_R of the yearly cumulated MIAWRARA ~~baselines~~ measurement noise together with the fit of a normal distribution. We find irrelevant changes between the different years and the maxima of the normal distribution fits are always centered at 0 K. The temperature fluctuations of the baselines range are in general between $-3 \cdot 10^{-2}$ and $3 \cdot 10^{-2}$ K. Alltogether it shows indirectly that the fitting of the baseline during the retrieval process is correct and stable.

Beside baseline artifacts which are not fitted correctly, it is known that the retrieval averaging kernels $\mathbf{A}$ can have an impact on the H_2O profile product. For a long-term measurement-based trend study it is of importance that any variability of $\mathbf{A}$ does not imply a data drift, which could induce an artificial trend. Accordingly we investigate this issue by a sensitivity trend test in Section 3.1.

2.2 H_2O data and error handling

Figure 2 presents the derived monthly mean H_2O data time series from the MIAWARA instrument at the northern mid-latitude observation site Bern. From 2007-04-01 to 2018-04-30 a total of 133 months are available. The white horizontal lines indicate the pressure level where the measurement response drops below 80 %. The annual cycle of water vapor can be seen in the plot and mainly originates from dynamics. In the summer mid-latitude mesosphere an upwelling motion of air with higher

H_2O mixing ratios determines the seasonal variability. The photodissociation by Lyman-α radiation which is stronger during summer has only a minor impact on the abundance of water vapor. This is predominantly the case in the upper mesosphere.

For the trend model it is very important to assess a reasonable uncertainty of the microwave radiometer measurements and thus the overall error of the monthly mean water vapor profiles. Two different types of errors were considered. The first type is the natural variability, which can be approximated by the standard error σ_{std} of the monthly mean H_2O profiles. The second type is the instrument related observational error σ_{obs} that belongs to the random error and depends on the thermal noise on the water vapor spectra. The observational error is calculated during the retrieval computation. Both errors were then combined in the following way to get a total monthly mean error profile σ_{tot} for the initialization of the trend model:

$$\sigma_{tot} = \sqrt{\sigma_{std}^2 + \sigma_{obs}^2} \tag{1}$$

The third panel (c) of Fig. 3 shows the temporal evolution of the total error at an altitude of $70\,\mathrm{km}$. At this altitude the error predominantly fluctuates around $0.3\,\mathrm{ppm}$.

3 Trend model description

We performed the trend analyses of the water vapor data through a robust multilinear parametric trend estimation method developed by von Clarmann et al. (2010). The trend program finds a linear trend of the data time series by minimizing a cost function.

The cost function includes a quadratic norm of the residual between a regression model and the analyzed monthly H_2O profile time series, weighted by the inverse covariance matrix of the data errors. The data errors are based on the monthly standard deviation and observational errors of the instruments as described in Sect. 2.2. In addition, error correlations between data points are supported which makes the method suitable for consideration of auto-correlated residuals. The regression function $Y(t)$ itself consists of an axis intercept, a linear trend, sine waves, and different proxies:

$$\begin{aligned} Y(t) = {} & a + b \cdot t + c_1 \cdot qbo_1(t) + d_1 \cdot qbo_2(t) \\ & + e \cdot F_{10.7}(t) + f \cdot MEI(t) \\ & + \sum_{n=2}^{m=3} \left[c_n \cdot sin\left(\frac{2\pi \cdot t}{l_n}\right) + d_n \cdot cos\left(\frac{2\pi \cdot t}{l_n}\right) \right] \end{aligned} \tag{2}$$

where t represents the time, a and b the constant term and the slope of the fit. The terms qbo_1 and qbo_2 are the normalized Singapore winds at 30 and $50\,\mathrm{hPa}$ pressure levels as provided by the Free University of Berlin via http://www.geo.fu-berlin.de/met/ag/strat/produkte/qbo/index.html. According to Kyrölä et al. (2010), the Singapore zonal wind series at the two altitudes are in good approximation orthogonal to each other so that the combination of both can reproduce the Quasi-Biennial Oscillation (QBO) phase shift. Fitting against the solar irradiance variability is accounted for by the $F_{10.7}$ flux which is a good proxy for this variability. The MEI term in the regression function is the Multivariate ENSO index. It describes the strength of the El Niño - Southern Oscillation (ENSO) with six parameters consisting of surface winds (zonal and meridional), sea surface

temperature, sea level pressure, surface air temperature and the sky cloudiness fraction. Both, the solar activity and MEI index lists are available from the following webpage: www.esrl.noaa.gov/psd/data/climateindices/list.

The sum term consists of two sine and cosine functions with the period length l_n, including the annual and semi-annual oscillations ($l_1 = 182.5\,\mathrm{d}$ and $l_2 = 365\,\mathrm{d}$). All coefficients (a, b, c_1, c_2, c_3, d_1, d_2, d_3, e and f) are fitted against the water vapor monthly mean time series in order to estimate the linear variations.

For the water vapor trend analyses, the multi-linear regression model needs the monthly mean profiles together with their uncertainties as input. Figure 3a represents the H_2O model fit (magenta line) on top of the monthly mean time series (blue line) derived by MIAWARA and the linear variation (black line) on $0.04\,\mathrm{hPa}$. Overall, the temporal H_2O variability could be very well reproduced by the model fit, which is also revealed by the residual between the measurements and fit (Fig. 3b) rarely exceeding $0.5\,\mathrm{ppm}$. Overall, the regression model is able to explain about 90 % of the variance of the measurements between 0.02 and 3 hPa. The three other panels display the H_2O fitted signals of the QBO (green line), solar F10.7 cm flux (red line) and ENSO (cyan line) proxies at $0.04\,\mathrm{hPa}$ ($70\,\mathrm{km}$).

3.1 Averaging kernel sensitivity test

Here we describe a performed test on an artificial water vapor profile time series in order to check if the variability of the MIAWARA averaging kernels can induce a data drift that might be misinterpreted as a trend. The averaging kernel matrix $\mathbf{A}$ is defined as

$$\mathbf{A} = \frac{\partial \hat{\mathrm{x}}}{\partial \mathrm{x}} = \frac{\partial \hat{\mathrm{x}}}{\partial \mathrm{y}} \frac{\partial \mathrm{y}}{\partial \mathrm{x}}. \tag{3}$$

It represents the sensitivity of the retrieved state $\hat{x}$ to the difference in the true atmospheric state x. The measured microwave spectrum is denoted as y. In our case we use a time series of one constant artificial H_2O profile x_{art} of $5\,\mathrm{ppm}$ at 50 pressure levels between 10 and $0.01\,\mathrm{hPa}$ at the same time steps as the original MIAWARA profiles were

$$\hat{x}_{art} = x_a + \mathbf{A} \cdot (\mathrm{x_{art}} - \mathrm{x_a}). \tag{4}$$

$\mathbf{A}$ has to be given on the grid of x_a and is interpolated to the grid of x, conserving the measurement response. The artificial convolved water vapor time series $\hat{x}_{art}$ (2007-04 to 2018-04) was then used to calculate monthly mean profiles that could be used as input to the trend model described in Section 3. No significant trend has been generated by the convolution process with the MIAWARA v301 averaging kernels, the retrieval version for the main trend analysis. In conclusion this means that the variability of $\mathbf{A}$ has no effect on the result of the trend estimate presented in Section 3.2.

3.2 H_2O trend estimate

After having shown that MIAWARA is measuring with a high instrumental stability, we are confident to present the trend result from the multi-linear parametric trend model (von Clarmann et al., 2010). Figure 4 shows the estimated water vapor trend profiles in absolute (left) and relative (right) values. The latter is calculated relative to the mean H_2O profile between April 2007 and ~~Mai~~ May 2018. Although the pressure range of the trend profile goes from 0.01 to $10\,\mathrm{hPa}$ in the two plots,

equivalent to 30-80 km, we restrict the trustworthy trend results to the altitudes of the MIAWARA radiometer which are to a degree of 80 % a priori independent. These lower and upper limits are marked by the horizontal red lines and are located at 0.03 and 2.5 hPa. At higher and lower altitudes the trend turns towards zero which is to be expected due to the fact that the MIAWARA mixing ratios gradually approach the climatology of Aura/MLS a priori values and those exhibit no long-term variability. Further not at every pressure level between the red lines a significant trend result could be obtained. This circumstance is expressed by the dashed green boxes by encompassing two altitude regions where the trend is two times larger than the uncertainty. ~~Accordant~~ According to Tiao et al. (1990) this is equivalent to a significance on the 95 % confidence level.

Below the stratopause from 1 to 2.5 hPa (42-48 km) a small but still significant negative trend, maximizing at 2 hPa could be determined. A mean linear decline rate of $-2.5 \cdot 10^{-3}\,\mathrm{ppm\,month^{-1}}$ results in $-0.3 \pm 0.1\,\mathrm{ppm\,decade^{-1}}$ (in relative units: $-4 \pm 1.2\,\%\,\mathrm{decade^{-1}}$) or a total loss of $\approx 0.33\,\mathrm{ppm}$ in the analyzed measurement period. This result is contradictory to explanations presented in North et al. (2015), where the increase of methane in the last decades is expected to also increase the water vapor content in the stratosphere by photodissociation and oxidation. On the other hand it has been pointed out, that the current understanding of the total stratospheric water vapor budget and the involved mechanisms controlling the entry and mixing of H_2O into the lower stratosphere are still under investigation.

The second statistically significant pressure layer in the MIAWARA trend profile is located in the mesosphere between 0.03 and 0.15 hPa (61-72 km). Although the 1σ error in the trend estimate is roughly doubled, the negative trend is clearly strengthened to $-0.6 \pm 0.2\,\mathrm{ppm\,decade^{-1}}$ at 0.03-0.04 hPa. In relative terms, we see a decrease between -12 to $-12.5 \pm 3\,\%\,\mathrm{decade^{-1}}$. The impact of the included extra month of H_2O data on the trend estimate was found to be below a change of ± 0.05 ppm. It is difficult to find other water vapor trend studies in the literature that investigate mesospheric altitudes and cover a comparable time period. Satellite data from Aura/MLS, which exist since August 2004, could be a basis for trend investigations. Lately MLS data has been globally analyzed by Froidevaux et al. (2018) and in case of water vapor a positive trend was derived between 100 and 0.03 hPa for northern and southern latitudes up to 60 degree. However, Aura/MLS H_2O data below 20 hPa could be problematic for estimating trends due to detected data drifts (Hurst et al., 2016).

4 Conclusions

Robust measurements by the water vapor radiometer MIAWARA, which belongs to the NDACC network, were performed between April 2007 and ~~Mai~~ May 2018 and used to obtain a middle atmospheric trend profile by means of a multi-linear parametric regression trend model fit of prior derived monthly mean profile and uncertainty data time series.

With this study, we demonstrated the high stability of the MIAWARA measurement noise within the 80 MHz ~~baseline~~ bandwidth and outlined that a potential variability of the averaging kernels does not induce a measurement drift. Hence we rely on the computed trend results with the presented multi-linear parametric regression trend model. Overall two altitude regions exhibit a significant (95 % confidence) negative water vapor trend during the time period of April 2007 to May 2018:

- 0.03-0.15 hPa (61-72 km): -12 to $-12.5 \pm 3\,\%\,\mathrm{decade^{-1}}$

- 1-2.5 hPa (42-48 km): $-4 \pm 1.2\,\%\,\mathrm{decade}^{-1}$

We are not able to give an explanation towards the reasons for the detected H_2O decline below the stratopause and in the mesosphere. The complexity of interactions between dynamics and chemistry is hardly addressable by observations alone. Numerical investigations will be needed to unravel the impacts of the different processes.

The fact that a lot of inconsistent results are published, regarding the evolution of middle atmospheric water vapor, it will be of great importance to continue with measurements from various ground-based observation sites. Although satellite missions, like EOS Aura, can provide data for almost the whole globe (82° S to 82° N), however the maintenance of the long-term stability and lifetime is limited and complicates trend studies.

Data availability. Data from the ground-based microwave instrument MIAWARA is publicly available from the NDACC database as monthly files with a diurnal temporal resolution (ftp://ftp.cpc.ncep.noaa.gov/ndacc/station/bern).

Competing interests. The authors declare that no competing interests are present.

Acknowledgements. The presented study is supported by the Swiss National Science Foundation Grant 200020-160048 and MeteoSwiss in the frame of the GAW project "Fundamental GAW parameters measured by microwave radiometry".

References

Ball, W. T., Alsing, J., Mortlock, D. J., Staehelin, J., Haigh, J. D., Peter, T., Tummon, F., Stübi, R., Stenke, A., Anderson, J., Bourassa, A., Davis, S. M., Degenstein, D., Frith, S., Froidevaux, L., Roth, C., Sofieva, V., Wang, R., Wild, J., Yu, P., Ziemke, J. R., and Rozanov, E. V.: Evidence for a continuous decline in lower stratospheric ozone offsetting ozone layer recovery, Atmospheric Chemistry and Physics, 18, 1379–1394, https://doi.org/10.5194/acp-18-1379-2018, https://www.atmos-chem-phys.net/18/1379/2018/, 2018.

Brasseur, G. and Solomon, S.: Aeronomy of the Middle Atmosphere: Chemistry and Physics of the Stratosphere and Mesosphere, vol. 32, Springer, 2006.

Buehler, S. A., Mendrok, J., Eriksson, P., Perrin, A., Larsson, R., and Lemke, O.: ARTS, the Atmospheric Radiative Transfer Simulator – version 2.2, the planetary toolbox edition, Geoscientific Model Development, 11, 1537–1556, https://doi.org/10.5194/gmd-11-1537-2018, https://www.geosci-model-dev.net/11/1537/2018/, 2018.

Deuber, B., Haefele, A., Feist, D. G., Martin, L., Kämpfer, N., Nedoluha, G. E., Yushkov, V., Khaykin, S., Kivi, R., and Vomel, H.: Middle Atmospheric Water Vapour Radiometer - MIAWARA: Validation and first results of the LAUTLOS / WAVVAP campaign, J. Geophys. Res., 110, D13 306, https://doi.org/10.1029/2004JD005543, 2005.

Eckert, E., von Clarmann, T., Kiefer, M., Stiller, G. P., Lossow, S., Glatthor, N., Degenstein, D. A., Froidevaux, L., Godin-Beekmann, S., Leblanc, T., McDermid, S., Pastel, M., Steinbrecht, W., Swart, D. P. J., Walker, K. A., and Bernath, P. F.: Drift-corrected trends and periodic variations in MIPAS IMK/IAA ozone measurements, Atmospheric Chemistry and Physics, 14, 2571–2589, https://doi.org/10.5194/acp-14-2571-2014, https://www.atmos-chem-phys.net/14/2571/2014/, 2014.

Eriksson, P., Jiménez, C., and Buehler, S. A.: Qpack, a general tool for instrument simulation and retrieval work, J. Quant. Spectrosc. Radiat. Transfer, 91, 47–64, https://doi.org/10.1016/j.jqsrt.2004.05.050, 2005.

Farman, J. C., Gardiner, B. G., and Shanklin, J. D.: Large losses of total ozone in Antarctica reveal seasonal ClOx/NOx interaction, Nature, 315, 207 EP –, https://doi.org/10.1038/315207a0, 1985.

Froidevaux, L., Kinnison, D. E., Wang, R., Anderson, J., and Fuller, R. A.: Evaluation of CESM1 (WACCM) free-running and specified-dynamics atmospheric composition simulations using global multi-species satellite data records, Atmospheric Chemistry and Physics Discussions, 2018, 1–70, https://doi.org/10.5194/acp-2018-546, https://www.atmos-chem-phys-discuss.net/acp-2018-546/, 2018.

Held, I. M. and Soden, B. J.: WATER VAPOR FEEDBACK AND GLOBAL WARMING, Annual Review of Energy and the Environment, 25, 441–475, https://doi.org/10.1146/annurev.energy.25.1.441, 2000.

Hurst, D. F., Oltmans, S. J., Vömel, H., Rosenlof, K. H., Davis, S. M., Ray, E. A., Hall, E. G., and Jordan, A. F.: Stratospheric water vapor trends over Boulder, Colorado: Analysis of the 30 year Boulder record, Journal of Geophysical Research: Atmospheres, 116, https://doi.org/10.1029/2010JD015065, 2011.

Hurst, D. F., Read, W. G., Vömel, H., Selkirk, H. B., Rosenlof, K. H., Davis, S. M., Hall, E. G., Jordan, A. F., and Oltmans, S. J.: Recent divergences in stratospheric water vapor measurements by frost point hygrometers and the Aura Microwave Limb Sounder, Atmospheric Measurement Techniques, 9, 4447–4457, https://doi.org/10.5194/amt-9-4447-2016, https://www.atmos-meas-tech.net/9/4447/2016/, 2016.

Kämpfer, N., Nedoluha, G., Haefele, A., and De Wachter, E.: Microwave Radiometry, vol. 10 of *ISSI Scientific Report Series*, Springer New York, https://doi.org/10.1007/978-1-4614-3909-7, 2012.

Kärcher, B.: Formation and radiative forcing of contrail cirrus, Nature Communications, 9, 1824, https://doi.org/10.1038/s41467-018-04068-0, 10.1038/s41467-018-04068-0, 2018.

Kiehl, J. T. and Trenberth, K. E.: Earth's Annual Global Mean Energy Budget, Bulletin of the American Meteorological Society, 78, 197–208, https://doi.org/10.1175/1520-0477(1997)078<0197:EAGMEB>2.0.CO;2, 1997.

Kyrölä, E., Tamminen, J., Sofieva, V., Bertaux, J. L., Hauchecorne, A., Dalaudier, F., Fussen, D., Vanhellemont, F., Fanton d'Andon, O., Barrot, G., Guirlet, M., Fehr, T., and Saavedra de Miguel, L.: GOMOS O_3, NO_2, and NO_3 observations in 2002–2008, Atmospheric Chemistry and Physics, 10, 7723–7738, https://doi.org/10.5194/acp-10-7723-2010, https://www.atmos-chem-phys.net/10/7723/2010/, 2010.

Lainer, M., Kämpfer, N., Tschanz, B., Nedoluha, G. E., Ka, S., and Oh, J. J.: Trajectory mapping of middle atmospheric water vapor by a mini network of NDACC instruments, Atmos. Chem. Phys., 15, 9711–9730, https://doi.org/10.5194/acp-15-9711-2015, 2015.

Lainer, M., Hocke, K., and Kämpfer, N.: Variability of mesospheric water vapor above Bern in relation to the 27-day solar rotation cycle, J. Atmos. Sol.-Terr. Phy., 143–144, 71–87, https://doi.org/10.1016/j.jastp.2016.03.008, 2016.

Lainer, M., Hocke, K., Rüfenacht, R., Schranz, F., and Kämpfer, N.: Quasi 18-hour wave activity in ground-based observed mesospheric H_2O over Bern, Switzerland, Atmospheric Chemistry and Physics Discussions, 2017, 1–29, https://doi.org/10.5194/acp-2016-1050, https://www.atmos-chem-phys-discuss.net/acp-2016-1050/, 2017.

Lainer, M., Hocke, K., and Kämpfer, N.: Long-term observation of mid-latitude quasi 2-day waves by a water vapor radiometer, Atmospheric Chemistry and Physics Discussions, 2018, 1–22, https://doi.org/10.5194/acp-2017-1150, https://www.atmos-chem-phys-discuss.net/acp-2017-1150/, 2018.

Liebe, H., Hufford, G., and Cotton, M.: Propagation modeling of moist air and suspended water/ice particles at frequencies below 1000 GHz, in: In AGARD, Atmospheric Propagation Effects Through Natural and Man-Made Obscurants for Visible to MM-Wave Radiation 11 p (SEE N94-30495 08-32), 1993.

Lossow, S., Hurst, D. F., Rosenlof, K. H., Stiller, G. P., von Clarmann, T., Brinkop, S., Dameris, M., Jöckel, P., Kinnison, D. E., Plieninger, J., Plummer, D. A., Ploeger, F., Read, W. G., Remsberg, E. E., Russell, J. M., and Tao, M.: Trend differences in lower stratospheric water vapour between Boulder and the zonal mean and their role in understanding fundamental observational discrepancies, Atmospheric Chemistry and Physics, 18, 8331–8351, https://doi.org/10.5194/acp-18-8331-2018, https://www.atmos-chem-phys.net/18/8331/2018/, 2018.

Moreira, L., Hocke, K., Eckert, E., von Clarmann, T., and Kämpfer, N.: Trend analysis of the 20-year time series of stratospheric ozone profiles observed by the GROMOS microwave radiometer at Bern, Atmospheric Chemistry and Physics, 15, 10 999–11 009, https://doi.org/10.5194/acp-15-10999-2015, https://www.atmos-chem-phys.net/15/10999/2015/, 2015.

Nedoluha, G. E., Kiefer, M., Lossow, S., Gomez, R. M., Kämpfer, N., Lainer, M., Forkman, P., Christensen, O. M., Oh, J. J., Hartogh, P., Anderson, J., Bramstedt, K., Dinelli, B. M., Garcia-Comas, M., Hervig, M., Murtagh, D., Raspollini, P., Read, W. G., Rosenlof, K., Stiller, G. P., and Walker, K. A.: The SPARC water vapor assessment II: intercomparison of satellite and ground-based microwave measurements, Atmospheric Chemistry and Physics, 17, 14 543–14 558, https://doi.org/10.5194/acp-17-14543-2017, https://www.atmos-chem-phys.net/17/14543/2017/, 2017.

North, G. R., Pyle, J., and Zhangi, F., eds.: Stratospheric Chemistry Topics: Stratospheric Water Vapor, Academic Press, Oxford, second edition edn., https://doi.org/10.1016/B978-0-12-382225-3.00393-5, 2015.

Rodgers, C. D.: Inverse methods for atmospheric sounding: theory and practice, vol. 2, World Scientific Publishing Co Pte. Ltd., 2000.

Sausen, R., Isaksen, I., Grewe, V., Hauglustaine, D., Lee, D. S., Myhre, G., Köhler, M. O., Pitari, G., Schumann, U., Stordal, F., and Zerefos, C.: Aviation radiative forcing in 2000: An update on IPCC (1999), Meteorologische Zeitschrift, 14, 555–561, https://doi.org/10.1127/0941-2948/2005/0049, 2005.

Scheiben, D., Tschanz, B., Hocke, K., Kämpfer, N., Ka, S., and Oh, J. J.: The quasi 16-day wave in mesospheric water vapor during boreal winter 2011/2012, Atmos. Chem. Phys., 14, 6511–6522, https://doi.org/10.5194/acp-14-6511-2014, 2014.

Steinbrecht, W., Froidevaux, L., Fuller, R., Wang, R., Anderson, J., Roth, C., Bourassa, A., Degenstein, D., Damadeo, R., Zawodny, J., Frith, S., McPeters, R., Bhartia, P., Wild, J., Long, C., Davis, S., Rosenlof, K., Sofieva, V., Walker, K., Rahpoe, N., Rozanov, A., Weber, M., Laeng, A., von Clarmann, T., Stiller, G., Kramarova, N., Godin-Beekmann, S., Leblanc, T., Querel, R., Swart, D., Boyd, I., Hocke, K., Kämpfer, N., Maillard Barras, E., Moreira, L., Nedoluha, G., Vigouroux, C., Blumenstock, T., Schneider, M., García, O., Jones, N., Mahieu, E., Smale, D., Kotkamp, M., Robinson, J., Petropavlovskikh, I., Harris, N., Hassler, B., Hubert, D., and Tummon, F.: An update on ozone profile trends for the period 2000 to 2016, Atmospheric Chemistry and Physics, 17, 10 675–10 690, https://doi.org/10.5194/acp-17-10675-2017, https://www.atmos-chem-phys.net/17/10675/2017/, 2017.

Stenke, A. and Grewe, V.: Simulation of stratospheric water vapor trends: impact on stratospheric ozone chemistry, Atmospheric Chemistry and Physics, 5, 1257–1272, https://doi.org/10.5194/acp-5-1257-2005, https://www.atmos-chem-phys.net/5/1257/2005/, 2005.

Tiao, G. C., Reinsel, G. C., Xu, D., Pedrick, J. H., Zhu, X., Miller, A. J., DeLuisi, J. J., Mateer, C. L., and Wuebbles, D. J.: Effects of autocorrelation and temporal sampling schemes on estimates of trend and spatial correlation, Journal of Geophysical Research: Atmospheres, 95, 20 507–20 517, https://doi.org/10.1029/JD095iD12p20507, https://agupubs.onlinelibrary.wiley.com/doi/abs/10.1029/JD095iD12p20507, 1990.

Trenberth, K. E., Dai, A., Rasmussen, R. M., and Parsons, D. B.: The Changing Character of Precipitation, Bulletin of the American Meteorological Society, 84, 1205–1218, https://doi.org/10.1175/BAMS-84-9-1205, 2003.

von Clarmann, T., Stiller, G., Grabowski, U., Eckert, E., and Orphal, J.: Technical Note: Trend estimation from irregularly sampled, correlated data, Atmospheric Chemistry and Physics, 10, 6737–6747, https://doi.org/10.5194/acp-10-6737-2010, https://www.atmos-chem-phys.net/10/6737/2010/, 2010.

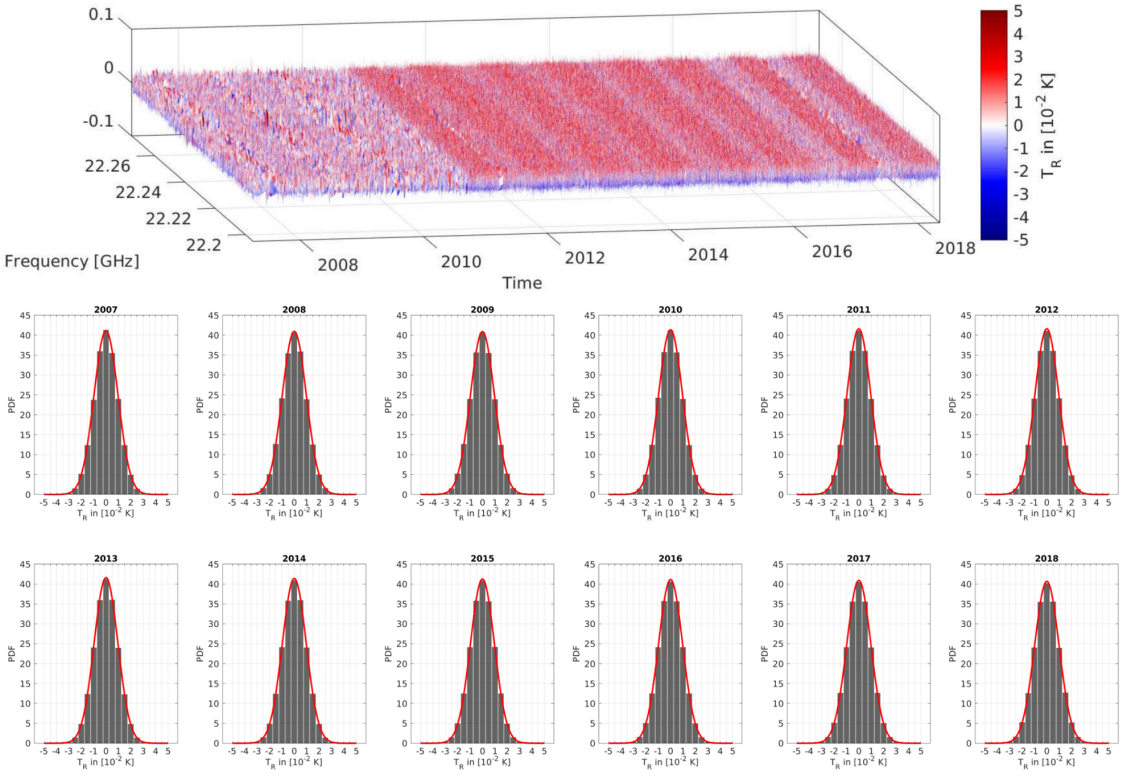

Figure 1. The 3-D plot in the top shows the temporal evolution of the MIAWARA ~~baseline~~ residuals (difference between measured difference spectrum and modeled spectrum) as residuum brightness temperature fluctuations T_R in $[10^{-2}\,\mathrm{K}]$ within the frequency range of $22.195\,\mathrm{GHz}$ to $22.275\,\mathrm{GHz}$ ($80\,\mathrm{MHz}$ bandwidth) from 2007 to 2018.

Yearly averaged histograms, showing the evolution of the PDF (probability density function) of the ~~MIAWARA baseline~~residuals, are presented below. The red curve is the fit of the corresponding normal distribution. The chosen bin width is $5 \cdot 10^{-3}\,\mathrm{K}$.

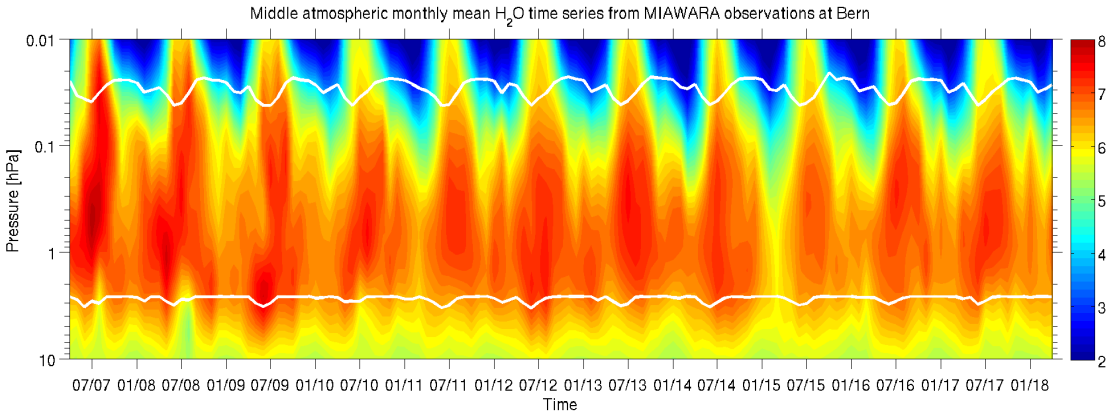

Figure 2. Monthly mean water vapor time series in $[\mathrm{ppm}]$ obtained by the MIAWARA instrument located at the Zimmerwald observatory near Bern between April 2007 and ~~Mai~~ May 2018. The horizontal upper and lower white lines indicate the pressure layer within which the measurement response is higher than $80\,\%$. This data set is used as input for the trend model.

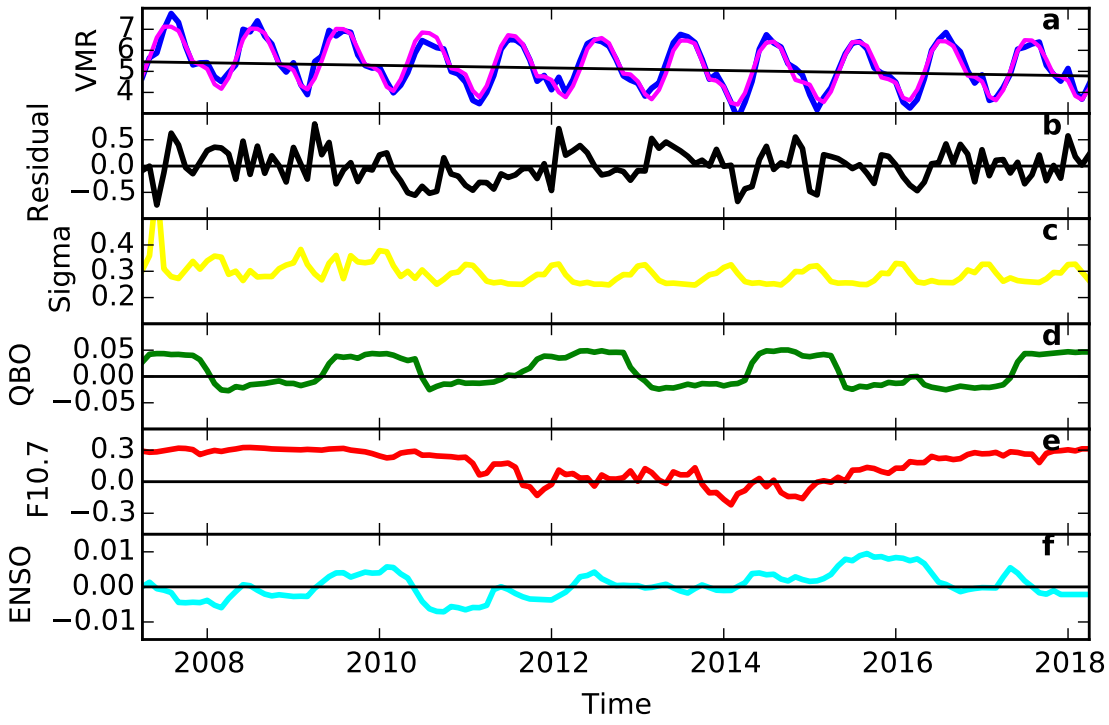

Figure 3. Panel (a) shows the trend fit at $0.04\,\mathrm{hPa}$ ($70\,\mathrm{km}$), with the MIAWARA monthly mean H_2O data (blue line), the calculated model fit (magenta line) and the related linear trend (black line). Panel (b) shows the residual and in the following panels (c), (d), (e) and (f) the evolution of the σ uncertainty (yellow line), the fitted signals of the QBO (green line), solar F$10.7\,\mathrm{cm}$ flux (red line) and ENSO (cyan line) proxies at $0.04\,\mathrm{hPa}$.

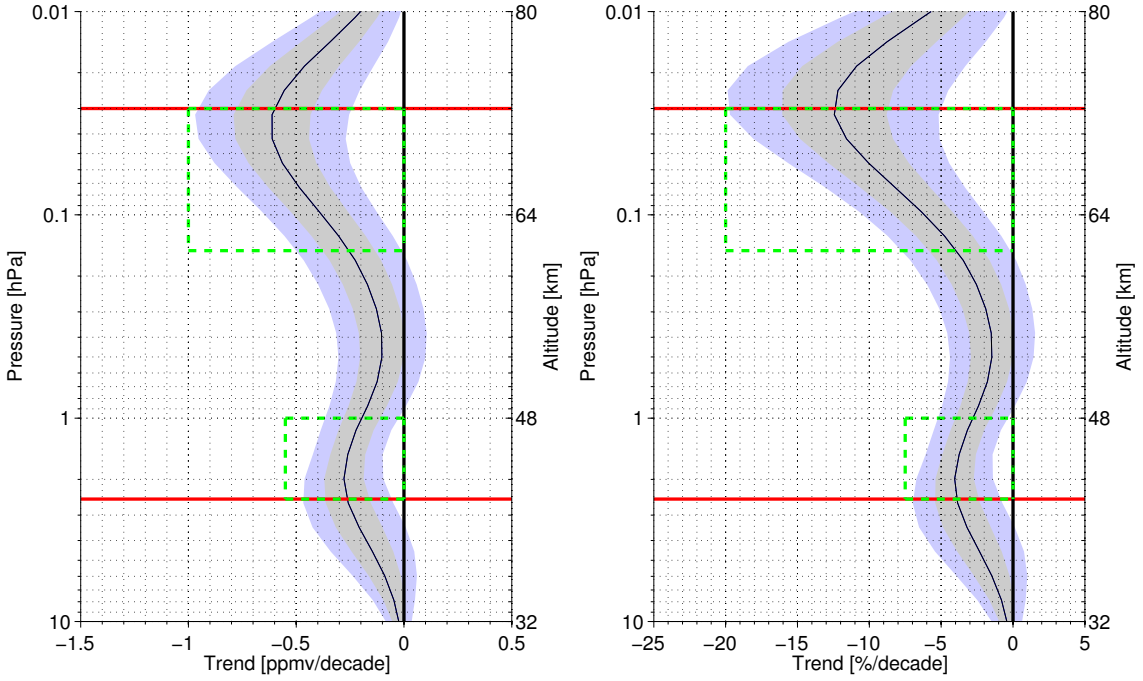

Figure 4. Estimated water vapor trend profile in $\left[\mathrm{ppm\,decade^{-1}}\right]$ (left), respectively $\left[\%\,\mathrm{decade^{-1}}\right]$ (rigth), for the time period between April 2007 and ~~Mai~~ May 2018 observed by the MIAWARA instrument at the Zimmerwald observatory close to Bern, Switzerland. The black line represents the trend profile; the grey and violet shaded areas represent the 1σ and 2σ uncertainties of the trend estimate. The green boxes show where the trend is statistically significant on the $95\,\%$ confidence level. The horizontal red lines mark the pressure range (0.03-$2.5\,\mathrm{hPa}$) where the MIAWARA data is to $\sim 80\,\%$ a priori independent.